

Transition-pathway models of atomic diffusion on fcc metal surfaces. I. Flat surfaces

Sung Youb Kim

Department of Mechanical Engineering, Korea Advanced Institute of Science and Technology, Daejeon 305-701, Korea

In-Ho Lee

Korea Research Institute of Standards and Science, Daejeon 305-600, Korea

Sukky Jun*

Department of Mechanical Engineering, University of Wyoming, Laramie, Wyoming 82071, USA

(Received 7 June 2007; published 10 December 2007)

Numerical calculation of minimum-energy paths and activation energy barriers for various atomic diffusion processes on fcc metal surfaces are presented. The computational method employed is the action-derived molecular dynamics that searches the approximate Newtonian trajectory on potential-energy surfaces. The minimization of a modified action, which facilitates the conservation of total energy and the control of kinetic energy, enables us to find efficiently the minimum-energy paths of complex microscopic processes. Diverse diffusion mechanisms on flat fcc substrates are investigated in this first part of the series. More complicated systems including surface steps are simulated in paper II.

DOI: [10.1103/PhysRevB.76.245407](https://doi.org/10.1103/PhysRevB.76.245407)

PACS number(s): 68.35.Fx, 68.47.De, 82.20.Kh, 02.70.Ns

I. INTRODUCTION

Although Fick's laws of diffusion account for diverse transport processes, they do not apply to the diffusive motion of a few atoms. Instead, in the context of harmonic transition-state theory, atomic diffusion can be properly described by the diffusion rate in terms of the energy barriers associated with the atomic trajectory of diffusion.¹ The activation energy barrier E_b is a factor of the diffusion rate Γ in the Arrhenius-type equation given as

$$\Gamma = \Gamma_0 \exp\left(-\frac{E_b}{k_B T}\right), \quad (1)$$

where k_B is the Boltzmann constant and T the temperature of the systems. Γ_0 is a prefactor and has different values according to materials and shapes of the system. Equation (1) has been popularly referred to as an estimate of the diffusion rates at low temperatures. Therefore, the diffusion rate at the atomic scale is a function of the activation energy barrier, temperature, and prefactor. The fundamental information on the energetics of a diffusion process can be obtained by the study of activation energy and transition path on potential-energy surfaces. On the other hand, the real dynamics of the process can be analyzed by fully considering the prefactor Γ_0 in addition to other factors. It is obvious that the diffusion rate is closely related to the diffusion coefficient in Fick's law, which is regarded as one of the material's properties at the continuum scale. However, the precise description of the relation between the diffusion rate and the coefficient still needs more work, although some equations have been proposed.² In experiments, even if we are able to observe individual atoms by virtue of scanning probe microscopy, it is, in general, difficult to capture the diffusive movements of adatoms on the substrate of the same species. The duration of the diffusion process is too short to observe atomic motions directly from an experiment. Furthermore, it is impossible to tell which atom actually moves into the current position

when both adatoms and substrate atoms are of the same species. Therefore, adatom diffusions have often been analyzed by computer simulations.

Atomic surface diffusion is a typical example of rare events in which multiple time scales are involved. First, the smallest time scale is the order of femtoseconds related to the vibrational frequency of an atom. The second one is the duration of atomic movement during a diffusion process, which is usually more than picoseconds so that its magnitude is in the order several times larger than atomic vibrational period. However, the most sophisticated point in diffusion simulations is that we do not know exactly when a particular diffusion event will occur. If we employ the conventional molecular dynamics (MD) simulations for a specific diffusion process, we have no choice but to wait until the process happens. In addition, even though some events may occur, there is no guarantee that the atom moves to the position along the minimum-energy path from which we expected to calculate the energy barrier. Therefore, it is not straightforward for a conventional MD simulation to simulate many cases of atomic surface diffusions.¹ This limitation becomes clearer when involving several atoms together in a complicated diffusion process. In conventional MD simulations, it is very difficult to compute its minimum-energy path for a concerted motion where several atoms move *collectively*.

On the other hand, the action-derived molecular dynamics (ADMD), proposed by Passerone and Parrinello,³ can provide an effective algorithm to search the transition pathways of an individual diffusion process considered. The method suggests a modified action to minimize in finding dynamic pathways that approximately fulfill the conditions of Newtonian trajectory. ADMD enables us to evaluate the accurate activation energy barrier along the minimum-energy path because it premises the given initial and final configurations. Therefore, a need arises that various processes in atomic surface diffusions should be analyzed by ADMD.

In this work of ADMD simulation, we search the minimum-energy paths and calculate the associated activa-

tion energy barriers, when one or more adsorbates diffuse on the substrate of a face-centered cubic (fcc) crystal structure. In this paper, we first focus on relatively well known diffusive motions on the flat surfaces because our primary purpose is to verify the effectiveness of ADMD simulation for surface diffusions. The diffusion energy barriers for single-atom hopping and exchange processes are examined. We employ six fcc metals, i.e., Ni, Cu, Pd, Ag, Pt, and Au. For surface orientations, three low Miller indices, i.e., (001), (111), and (110), are considered. The calculations for the concerted motions of two, three, and four adparticles are next performed. Further studies on the diffusion mechanisms associated with steps and step corners on the substrates are investigated in paper II.⁴

This paper is presented as follows. The formulation of ADMD method is briefly introduced in Sec. II. Next, in Sec. III, the activation energy barriers of single-atom diffusion on flat surfaces are investigated in comparison with a large amount of data available from literature. The collective motions of two or more adatoms on flat surfaces are discussed in Sec. IV. Finally, conclusions are presented in Sec. V.

II. COMPUTATIONAL METHODOLOGY

The action-derived molecular dynamics is based on the least action principle.³ By minimizing the classical action, we can search for the minimum-energy path connecting given initial and final atomic configurations. The discretized form of the action is written as

$$S^h = \sum_{j=0}^{P-1} \Delta \left[\sum_{l=1}^N \frac{m_l}{2\Delta^2} (\mathbf{q}_j^l - \mathbf{q}_{j+1}^l)^2 - V(\{\mathbf{q}_j\}) \right], \quad (2)$$

where the time domain is discretized into P intervals, $\Delta = \tau/P$. At a time step j , the corresponding atomic configuration, which is called image, bead, or replica, is abbreviated by the $3N$ dimensional vector, $\{\mathbf{q}_j\}$. m_l is the mass of the l th atom, and \mathbf{q}_j^l denotes the position vector of the l th atom at the j th image. The path $\mathbf{q}(t)$ in the configurational space is represented by its discrete values at the initial \mathbf{q}_0 and final states \mathbf{q}_P , and those at the intermediate time levels $t_1, t_2, \dots, t_j, \dots, t_{P-1}$, which are denoted by $\mathbf{q}_1, \mathbf{q}_2, \dots, \mathbf{q}_j, \dots, \mathbf{q}_{P-1}$. The stationarity condition $\delta S^h = 0$ will lead to a set of linear equations.

However, the discretized pathway obtained from the minimization of Eq. (2) does not exactly satisfy the total-energy conservation. Furthermore, it is not tractable, in practice, to find accurate Verlet trajectories directly from Eq. (2) because the given discretized action is not bounded. In order to find effectively the accurate energy-conserving minimum-energy pathway, Passerone and Parrinello³ introduced a constraint term to the original discretized action of Eq. (2), resulting in a new discretized object function to be minimized. They proposed the modification of the original discretized action as

$$\Theta(\{\mathbf{q}_j\}, E) = S^h + \mu_E \sum_{j=0}^{P-1} (E_j - E)^2, \quad (3)$$

where the total energy at the j th image is given as

$$E_j = K_j + V_j = \sum_{l=1}^N \frac{m_l}{2\Delta^2} (\mathbf{q}_j^l - \mathbf{q}_{j+1}^l)^2 + V(\{\mathbf{q}_j\}). \quad (4)$$

Along the pathway, the total energy can therefore be controlled to be close to the pre-determined target value of E due to the penalty term in Eq. (3) with an appropriate selection of parameter μ_E .^{3,5}

Lee *et al.*⁶ have shown that the pathway quality can further be improved by introducing additional conditions such as

$$\Phi(\{\mathbf{q}_j\}, E; T) = \Theta(\{\mathbf{q}_j\}, E) + \mu_K \sum_{l=1}^N \left(\langle K_l \rangle - \frac{3k_B T}{2} \right)^2, \quad (5)$$

where $\langle K_l \rangle$ represents the averaged kinetic energy of the l th atom along the trajectory.⁶ Together with the penalty parameter μ_K , the fictitious temperature T is also a computational parameter to control the kinetic energy of the system. In terms of the value of the Onsager-Machlup action, it has been shown that the quality of pathways are enhanced by introducing the term of fictitious temperature.⁶ Consequently, a better pathway model, which is closer to the Newtonian trajectory and has lower activation energy, can be exploited if the additional penalty function is properly employed in the pathway optimization procedure. Throughout this series of papers, we use the discretized action with kinetic-energy control, as in Eq. (5). ADMD has been used for diverse application problems such as structural transformation of nanomaterials, chemical reaction and autocatalysis, protein folding, and dislocation dynamics.⁷⁻¹⁵

In this work, the interactions between metal atoms are described by the tight-binding second-moment approximation (TB-SMA) potential proposed by Cleri and Rosato.¹⁶ This semiempirical many-body interatomic potential has been used in many surface diffusion studies such as the self-diffusion simulation on Pd(111) by MD simulation.¹⁷ Note that (semi-)empirical potentials, including the TB-SMA potential, employ fitted parameters, which are designed to reproduce the bulk properties such as cohesive energy and elastic constants. Therefore, in general, they are considered to be less accurate than first-principles calculations, based on the density functional theory, in describing the characteristics of nonbulky systems such as surfaces and interfaces. Nonetheless, these types of empirically based potentials are popularly adopted in many surface diffusion studies because they can facilitate the systems of a large number of atoms, which are otherwise difficult to simulate. It is also noted that different types of empirical potentials, such as the embedded atom method (EAM), may result in different values since fitting methods and reference data are not the same as those of the TB-SMA potential. For the simple cases of surface diffusion, comparative studies between TB-SMA and EAM potentials can be found elsewhere.^{2,18} Throughout this paper, we will compare our results with other available data that were obtained by different types of numerical methods and interatomic potentials. For example, in the simulation of Cu one-atom self-diffusion, we have verified that our results are sufficiently consistent with a recent report calculated by the nudged elastic band method with EAM potential.¹⁹

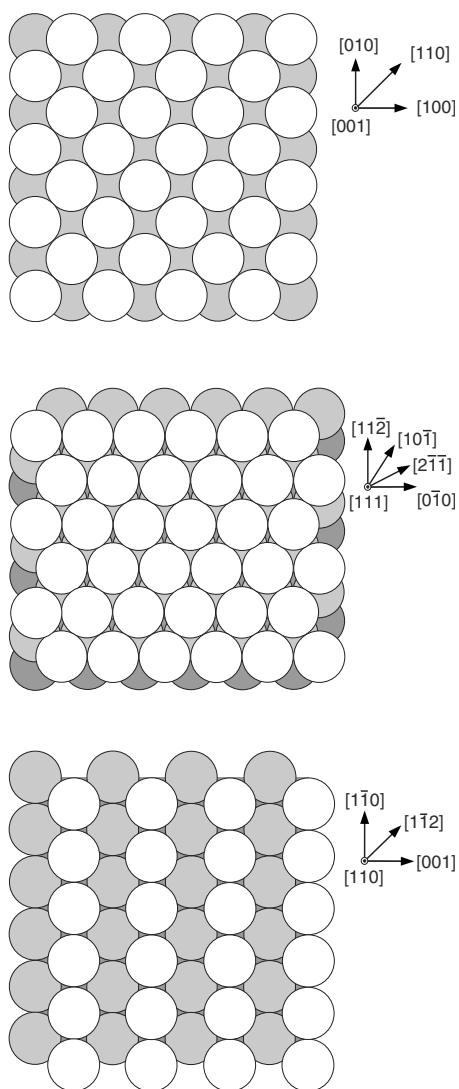


FIG. 1. Three flat surfaces of the fcc structure for diffusion simulations. From top to bottom: (001), (111), (110), surfaces.

III. SINGLE-ADATOM DIFFUSIONS ON FLAT SUBSTRATES

A. Simulation models

The activation energy barriers of single-adatom diffusions on flat surfaces are investigated in this section. Six metal species are considered in diffusing and substrate atoms, Ni, Cu, Pd, Ag, Pt, and Au in the order of atomic number. All of them form fcc crystal structures. We select three substrate orientations that have low Miller indices; (001), (111), and (110) surfaces are shown in Fig. 1 with lattice directions. These are the surfaces commonly observed in experiments.

For the (001) flat substrate, the model employed consists of six atomic layers of 50 atoms, and the total number of atoms is thus 300. We impose a periodic boundary condition (PBC) on the in-plane directions $[100]$ and $[010]$, and make a free surface by imposing a free boundary condition (FBC) on the out-of-plane direction $[001]$. Six atomic layers consisting of 36 and 48 atoms form the models of (111) and (110) flat substrates, respectively. A total of 216 and 288

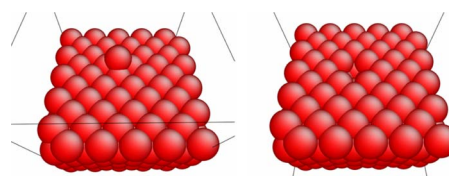


FIG. 2. (Color online) Models used in one atom diffusion on the (001) surface. Adatom diffusion model (left) and vacancy diffusion model (right).

atoms are employed. Again, PBC is imposed on the in-plane directions and FBC on the out-of-plane direction for both models. An extra atom is added onto the free surface for adatom diffusion simulations, as shown in Fig. 2. In this paper, perspective views of three dimensional atomic configurations were all visualized using the open software ATOM-EYE developed by Li.²⁰ A single vacancy is modeled by removing a substrate atom from the top layer, as depicted also in Fig. 2. Every model employed in this paper is carefully compared with twice or three times larger models in terms of the number of atoms, and they give nearly the same results. The initial and final configurations, both of which are local minima on the potential-energy surface, are fully relaxed by using an energy minimization scheme before conducting every ADMD calculation. We set the time step (i.e., the interval between two images) to 5 fs and use 200 (or 300 for some examples) images for each diffusion process.

B. Hopping and exchange mechanisms

Elementary movements in adatom diffusion are hopping and exchange. Typical diffusion routes by hopping and exchange on the (001) surface are shown in Fig. 3. Note that the final positions and traveled distances of the two motions are different. By hopping, the adatom travels the closest distance between local minima along the $\langle 110 \rangle$ direction, while, in exchange, it does the distance of lattice constant along the $\langle 100 \rangle$ direction. Exchange processes are relevant especially to homoepitaxial metallic systems.²

When an adatom is located at a local minimum on the (111) flat surface, there are three nearest neighboring local minima of which the potential energies are slightly higher than that of the adatom's original site. There are six second-nearest neighboring local minima of which the potential en-

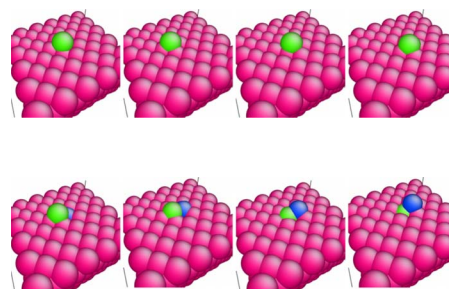


FIG. 3. (Color online) Basic diffusion pathways on the (001) surface. Hopping (top row) and exchange (bottom row) pathways. Each row proceeds from left to right.

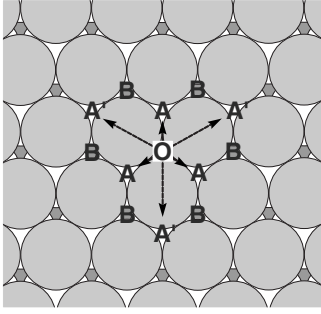


FIG. 4. Diffusion pathways of a single adatom on the (111) surface. Positions of local minima and diffusion paths.

ergies are the same as that of the original position. We indicate the nearest and the second-nearest neighboring local minima as A and B, respectively, in Fig. 4. The slight difference between the potential energies of A and B originates from the fault of stacking sequence on the (111) surface. Due to this profile, three hopping moves (from O to A) and three exchange moves (from O to A') are most probable on the (111) substrate, as illustrated in Fig. 4. The two mechanisms result in different final configurations from each other.

The (110) surface is highly anisotropic due to its atomic arrangement so that there are two distinct hopping routes. One is the so-called in-channel hopping where the adatom moves along the atomic valley to the $\langle 110 \rangle$ direction (from O to A as denoted in Fig. 5). The other is the out-channel hopping in which the adatom climbs over the atomic mountains to the $\langle 100 \rangle$ direction (from O to B). The exchange can occur along the $\langle 112 \rangle$ direction (from O to C). In Figs. 4 and 5, solid and dotted arrows represent the paths (and the final positions, too) of hopping and exchange movements, respectively. For the six atomic species considered, we employ only a (1×1) geometry for comparison purposes, even though (1×2) is known to be a more stable structure for Pt and Au.

The ADMD results of energy barriers of the six atomic species for hopping and exchange on the three flat substrates are summarized in Table I. In (001) surface models, hopping is the dominant mechanism for Ni, Cu, Pd, and Ag, but ex-

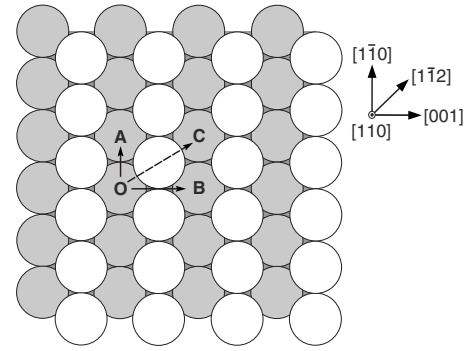


FIG. 5. Diffusion pathways of a single adatom on the (110) surface.

change is more favorable for Pt and Au. It is noted that the exchange barrier is almost four times greater than the hopping barrier in the case of Ni. While Ni has the lowest hopping barrier of 0.38 eV, Pt has the highest one of 0.87 eV. Therefore, the exchange mechanism is favorable for $5d$ metals (Pt and Au), while hopping is dominant for $3d$ (Ni and Cu) and $4d$ (Pd and Ag) metals.

The variation of the potential-energy surface for the (111) plane is smaller than those of other two planes because the (111) plane is the most closely packed one of fcc structures and is highly symmetric. Therefore, the (111) surface has very low hopping barriers and very high exchange barriers, as can be seen in Table I. For example, the exchange barrier of Cu is 1.35 eV, which is about 30 times larger than its hopping barrier. We may thus conclude that the diffusion of an adatom on the (111) surface occurs by hopping mechanism only.

Hopping movements onto a normal stacking site (B in Fig. 4) and a stacking fault site (A) reveal almost the same values of energy barrier for all atomic species considered, which suggests that jumps to the two different sites can occur with equivalent rate. However, it is the case when we take into account the energetics only. In reality, those two hopping paths possess many transition states in addition to the saddle point. These intermediate states are all different between the two trajectories. This effect is included in the prefactors of

TABLE I. Activation energy barriers (eV) of single-adatom self-diffusions on flat surfaces.

Surface	Mechanisms	Elements					
		Ni	Cu	Pd	Ag	Pt	Au
(001)	Hopping [110]	0.376	0.477	0.621	0.467	0.875	0.531
	Exchange [100]	1.304	0.708	0.725	0.624	0.802	0.388
(111)	Hopping $[11\bar{2}]$	0.061	0.043	0.109	0.064	0.171	0.117
	Hopping $[10\bar{1}]$	0.061	0.043	0.110	0.065	0.173	0.135
	Exchange $[2\bar{1}\bar{1}]$	1.633	1.352	1.315	1.126	1.627	0.861
(110)	In-channel Hopping $[1\bar{1}0]$	0.301	0.241	0.380	0.277	0.490	0.274
	Exchange $[1\bar{1}2]$	0.301	0.323	0.551	0.388	0.779	0.468
	Out-channel Hopping [001]	1.026	1.020	0.965	0.818	1.247	0.700

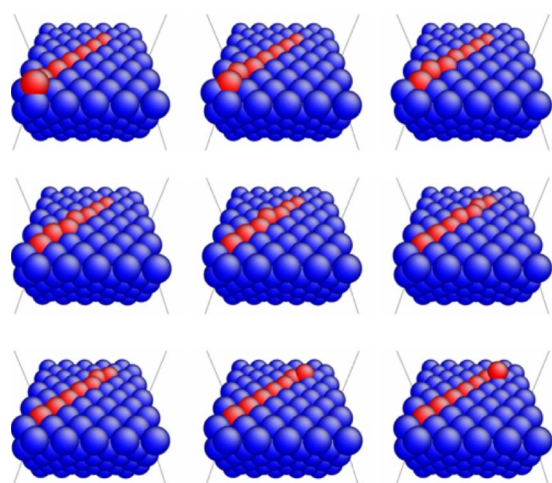


FIG. 6. (Color online) Multiple-exchange diffusion process on the Cu(001) surface. Nine snapshots along the diffusion pathway (top panel, proceeding from left to right and from top to bottom) and its energy profile (bottom panel).

Eq. (1). Consequently, the diffusion rates of the two jumps are not identical, in general.

In-channel hopping along the $[1\bar{1}0]$ direction on the (110) surface has a much lower barrier than out-channel hopping along $[001]$ for all species. For example, the out-channel hopping of the Cu adatom should overcome a four times higher energy barrier than the in-channel jump. This can be clearly noticed when we pay attention to the atomic arrangement on the flat (110) surface in the bottom of Fig. 1. According to Table I, exchange diffusion barriers are higher than that of in-channel hopping, but lower than that of out-channel hopping. As widely accepted, out-channel diffusion is exchange dominant for all cases. Ni is the only exception where in-channel hopping and exchange result in nearly the same diffusion barriers.

C. Comparison with other data in literature

Our primary objective in this paper is to demonstrate that ADMD is efficient for the calculation of transition pathways,

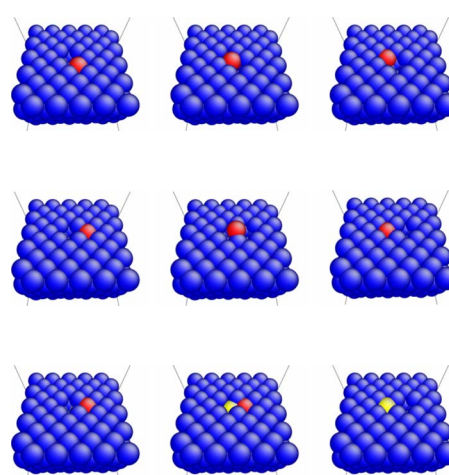


FIG. 7. (Color online) A vacancy diffusion on the (001) surface. “Hopping” type (top row), “hurdling” type (middle row), and “kicking out” type (bottom row). Each row proceeds from left to right.

particularly for very complex diffusion processes. On the other hand, hopping and exchange mechanisms in single-adatom self-diffusion on flat surfaces are the simplest ones so that their activation energies have been considerably studied by other numerical methods and experiments as well as the current method. In this subsection, we thus present comparisons of our ADMD results with other preexisting data from literature^{21–68} for these simple diffusive motions. We note that the comprehensive physics-based analysis of computed energy barriers from many different numerical methods is beyond the scope of this paper. Instead, we limit ourselves with stating the general tendency of previous data and comparing it with our simulation results. For this purpose of validation, Tables II–IV are given for (001), (111), and (110) surfaces, respectively. More complex diffusive motions, such as heterodiffusion and correlated movements, have been much less studied by other researchers due mainly to the lack of robust computational methods. Therefore, those data will occasionally be compared in the text, rather than in a separate table, throughout the subsequent sections.

As shown in Table II for the (001) surface, referential data are in reasonable agreement for Cu. The empirical potentials for Cu hopping range from 0.38 to 0.51 eV, and the current value (0.477 eV) falls within this range. The calculations based on density functional theory (DFT), using local density approximation (LDA) and generalized gradient approximation (GGA), lie between 0.52 and 0.75 eV, which are higher than empirical potentials. On the other hand, the activation energies of Cu exchange by empirical potentials and DFT are mostly 0.72–1.03 eV (except one case of 0.18 eV), which is also comparable with our result, 0.708 eV. We note that experimental observations of 0.28–0.40 eV are more comparable with the computed results of hopping rather than those of exchange. We can thus deduce that hopping is dominant over exchange for this case of Cu surface, which is supported by our ADMD calculation as well.

Ag and Ni cases have a fair amount of data available from literature, as many as the Cu case. Especially Ag diffusions

TABLE II. Comparison of activation energy barriers (eV) of single-atom self-diffusions on (001) flat surfaces.

Mechanism	Method	Ni	Cu	Pd	Ag	Pt	Au	
Hopping [110]	Present	0.376	0.477	0.621	0.467	0.875	0.531	
	Empirical	0.63 ^a	0.38 ^a	0.71 ^a	0.48 ^a	0.44 ^a	0.64 ^a	
	Potentials	0.68 ^b	0.53 ^b	0.74 ^b	0.48 ^b	1.25 ^b	0.84 ^b	
		0.60 ^c	0.51 ^c	0.73 ^c	0.46 ^c	0.36 ^l		
		0.67 ^d	0.46 ^d	0.64 ^d	0.40 ^d			
		0.63 ^e	0.40 ^e		0.37 ^e			
		0.30 ^f	0.39 ^h		0.48 ^k			
		0.53 ^g	0.44 ⁱ					
		0.68 ⁱ						
	LDA			0.75 ⁿ		0.52 ^p	1.23 ^r	0.83 ^s
				0.69 ^r		0.50 ^q		0.62 ^q
	GGA			0.52 ⁿ		0.45 ^p	1.03 ^r	0.58 ^s
	Exchange [100]	Present	1.304	0.708	0.725	0.624	0.802	0.388
Empirical		0.93 ^a	0.72 ^a	0.61 ^a	0.75 ^a	0.31 ^a	0.30 ^a	
Potentials		1.15 ^b	0.79 ^b	0.59 ^b	0.60 ^b	0.64 ^b	0.32 ^b	
		1.00 ^c	0.77 ^c	0.96 ^c	0.70 ^c	0.27 ^l		
		0.47 ^d	0.18 ^d	0.70 ^d	0.41 ^d			
		0.84 ^e	1.00 ^e	0.62 ^m	0.61 ^e			
			0.79 ^h		0.78 ^k			
LDA				1.03 ⁿ		0.93 ^p	0.48 ^r	0.65 ^s
				0.97 ^r				
GGA				0.96 ⁿ		0.73 ^p	0.39 ^r	0.40 ^s
Expt.		0.63 ^t	0.40 ^u	0.61 ^v	0.40 ^w	0.47 ^x		
		0.60 ^y	0.39 ^z		0.38 ^{aa}			
			0.28 ^{ab}					
			0.36 ^{ac}					

^aAdams-Foils-Wolfer (AFW) EAM in Ref. 21.^bVoter-Chen (VC) EAM in Ref. 21.^cCorrected effective medium (CEM) MD Monte Carlo (MC) in Ref. 22.^dCEM in Ref. 22.^eFBD EAM in Ref. 28.^fEffective medium (EM) in Ref. 23.^gMorse in Ref. 24.^hRosato, Guillopé, and Legrand (RGL)

TB-SMA in Ref. 25.

ⁱFoils, Baskes, and Daw (FBD) EAM in Ref. 27.^jSutton-Chen (SC) in Ref. 24.^kRGL TB-SMA in Ref. 26.^lVC EAM in Ref. 26.^mFoils EAM in Ref. 29.ⁿReference 30.^oReference 31.^pReference 32.^qReference 33.^rReference 34.^sReference 35.^tReference 36.^uReference 37.^vReference 38.^wReference 39.^xReference 40.^yReference 41.^zReference 42.^{aa}Reference 43.^{ab}Reference 44.^{ac}Reference 45.

reveal the tendency that is very similar to Cu. Empirical potentials for hopping mechanism result in 0.37–0.48 eV for energy barriers, and our result is 0.467 eV. They are slightly lower than DFT calculations (0.45–0.52 eV). Ag exchange is in the range of 0.60–0.93 eV, considering empirical potentials and DFT together (one exception is 0.41 eV). Our exchange result is also comparable to 0.624 eV. Again, experimental results of Ag (0.38 and 0.40 eV) suggest that hop-

ping is more probable than exchange, which is consistent with Cu cases. This remark applies to the case of Ni as well. In particular, most results of empirical potentials (0.53–0.68 eV, except one result of 0.30 eV) match very well with experimental observations (0.60 and 0.63 eV). Our calculation of Ni hopping results in a value (0.376 eV) less than most of other empirical potentials, while our exchange barrier (1.304 eV) is higher than others. Nonetheless, our

TABLE III. Comparison of activation energy barriers (eV) of single-adatom self-diffusions on (111) flat surfaces.

Mechanism	Method	Ni	Cu	Pd	Ag	Pt	Au
Hopping [$11\bar{2}$]	Present	0.061	0.043	0.109	0.064	0.171	0.117
Hopping [$10\bar{1}$]	Present	0.061	0.043	0.110	0.065	0.173	0.135
	Empirical	0.056 ^a	0.026 ^a	0.031 ^a	0.059 ^a	0.007 ^a	0.021 ^a
	Potentials	0.063 ^b	0.044 ^b	0.059 ^b	0.044 ^b	0.078 ^b	0.038 ^b
		0.06 ^c	0.05 ^c	0.04 ^c	0.04 ^c	0.07 ^c	0.04 ^c
		0.036 ^d	0.039 ^d	0.034 ^d	0.020 ^d	0.048 ^d	0.029 ^d
		0.049 ^e	0.043 ^e		0.119 ^j	0.176 ^e	0.112 ^e
		0.016 ^g	0.042 ^h		0.055 ⁱ	0.08 ^j	0.013 ^f
		0.086 ^m				0.038 ^j	
		0.063 ^m					
	LDA				0.14 ⁿ	0.150 ^o	0.22 ⁿ
					0.082 ^o	0.38 ^p	
						0.33 ^q	
						0.29 ^r	
	GGA				0.078 ^r		
Exchange [$2\bar{1}1$]	Present	1.633	1.352	1.315	1.126	1.627	0.861
	Empirical	2.050 ^e	1.455 ^e			2.105 ^e	0.878 ^e
	Potentials						
Expt.		0.33 ^t	0.04 ^u	0.35 ^v	0.097 ^w	0.25 ^q	
					0.15 ^x	0.160 ^w	
						0.26 ^y	
						0.26 ^z	

^aAFW EAM in Ref. 21.^bVC EAM in Ref. 21.^cVC EAM in Ref. 46.^dCEM MD/MC in Ref. 47.^eTB-SMA in Ref. 48.^fSurface embedded-atom method (SEAM) in Ref. 49.^gMorse in Ref. 24.^hRGL TB-SMA in Ref. 26.ⁱAFW EAM in Ref. 50.^jEAM in Ref. 51.^kSC in Ref. 24.^lCEM in Ref. 52.^mVC EAM in Ref. 26.ⁿReference 33.^oReference 53.^pReference 55.^qReference 56.^rReference 57.^sReference 54.^tReference 36.^uReference 58.^vReference 59.^wReference 60.^xReference 61.^yReference 62.^zReference 63.

results can still validate the above remark that hopping is more likely to occur than exchange.

In spite of limited available data for the other three cases of Pd, Pt, and Au, worthy of note is that these three cases do not demonstrate a clear preference of the hopping mechanism over the exchange movement. For example, the Pd hopping results of energy barriers span from 0.64 to 0.74 eV (our result is 0.621 eV), while the exchange barriers result in a wider range of 0.59–0.96 eV, including our value of 0.725 eV. Furthermore, the only experimental value for Pd, 0.61 eV, may comply with either mechanism. In addition, for

the cases of Pt and Au, the majority of reference data indicates that the exchange mechanism can possibly be more probable than the hopping diffusion, which can also be stated from our ADMD results, as seen in Table II.

Three diffusion mechanisms are considered for the (111) surface, as given in Table III. We have previously mentioned that from our ADMD results, the activation energies of exchange mechanism is extremely higher than those of hopping mechanism. This comment is clearly confirmed from all other data shown in Table III. One- or even two-order larger activation energy barriers are obtained from exchange diffu-

TABLE IV. Comparison of activation energy barriers (eV) of single-adatom self-diffusions on (110) flat surfaces.

Mechanism	Method	Ni	Cu	Pd	Ag	Pt	Au
Hopping [$1\bar{1}0$]	Present	0.301	0.241	0.380	0.277	0.490	0.274
	Empirical	0.44 ^a	0.23 ^a	0.28 ^a	0.32 ^a	0.25 ^a	0.25 ^a
	Potentials	0.39 ^b	0.28 ^b	0.30 ^b	0.25 ^b	0.53 ^b	0.34 ^b
		0.420 ^c	0.292 ^c	0.366 ^c	0.291 ^c	0.420 ^c	0.268 ^c
		0.18 ^d	0.08 ^d	0.30 ^d	0.26 ^d	0.64 ⁱ	0.28 ^d
		0.24 ^e	0.26 ^e	0.28 ^e	0.25 ^e	1.01 ^j	
	0.39 ^g	0.23 ^f		0.28 ^f			
		0.26 ⁱ					
Exchange [$1\bar{1}\bar{2}$]	Present	0.301	0.323	0.551	0.388	0.779	0.468
	Empirical	0.49 ^a	0.30 ^a	0.42 ^a	0.42 ^a	0.43 ^a	0.40 ^a
	Potentials	0.42 ^b	0.31 ^b	0.34 ^b	0.31 ^b	0.68 ^b	0.42 ^b
		0.564 ^c	0.419 ^c	0.599 ^c	0.561 ^c	0.809 ^c	0.554 ^c
		0.35 ^d	0.09 ^d	0.33 ^d	0.34 ^d	1.97 ⁱ	0.46 ^d
		0.40 ^f	0.49 ^f	0.38 ^f	0.33 ^f	1.09 ^g	
		0.29 ⁱ		0.38 ⁱ			
Out-channel hopping [001]	Present	1.026	1.020	0.965	0.818	1.247	0.700
	Empirical Potentials	1.157 ^c	0.826 ^c	0.776 ^c	0.639 ^c	0.945 ^c	0.670 ^c
Expt.		0.23 ^k				1.35 ^g	
		0.32 ⁿ				0.84 ^l	>0.38 ^m
						0.78 ^o	

^aEAM (AFW) in Ref. 21.^bVC EAM in Ref. 21.^cEM in Ref. 64.^dCEM in Ref. 65.^eMorse in Ref. 66.^fCEM MD/MC in Ref. 65.^gSC in Ref. 67.^hVC EAM in Ref. 26.ⁱRGL TB-SMA in Ref. 25.^jRGL TB-SMA in Ref. 26.^kHopping in Ref. 36.^lHopping in Ref. 66.^mReference 68.ⁿExchange in Ref. 36.^oExchange in Ref. 66.

sion simulations, compared with the activation energies of the two hopping moves. For [$10\bar{1}$] hopping, our ADMD values reside well within the variation of other numerical results for all of the six species. Our results are 0.061 eV (others, 0.016–0.086 eV) for Ni, 0.043 eV (0.026–0.05 eV) for Cu, 0.111 eV (0.031–0.059 eV) for Pd, 0.065 eV (0.020–0.14 eV) for Ag, 0.173 eV (0.007–0.38 eV) for Pt, and 0.135 eV (0.013–0.22 eV) for Ni, even though some cases demonstrate relatively wide ranges of values depending on the computational methods used. Especially, the DFT-based computation tends to result in higher activation barriers than empirical potentials, which has been recognized in some cases of previous (001) surfaces (Table II). For the [$2\bar{1}1$] exchange diffusion, only one reference is available, and its data are comparable with our results, as seen from Table III.

On the (110) surfaces, the in-channel hopping and the out-channel exchange are commonly more probable than the out-channel hopping, as discussed in previous subsections,

which is verified by the referential data provided in Table IV. Unlike previous two surfaces, most of the data obtained from empirical potentials for [$1\bar{1}0$] in-channel hopping barriers fall within a relatively narrow range of variation, except the corrected effective medium theory⁶⁵ for Ni and Cu. ADMD results also match well with these data. For example, the ADMD energy barrier of Ag is 0.277 eV, while others vary as 0.25–0.32 eV. For the [$1\bar{1}\bar{2}$] out-channel exchange, a similar tendency can also be seen from Table IV. For out-channel hopping, only one (two for Pt) reference is available and is also comparable with ADMD data for all of the six species. Experimental data for the (110) surface are very limited. However, we note that, for Ni, ADMD results of 0.301 eV are very close to an experimental data of 0.32 eV, and for Pt, our value of 0.779 (out-channel exchange) nearly equals to an experimental value of 0.78 eV.

D. Hopping diffusions in heteroepitaxial systems

We further simulate the hopping diffusions of the six individual adparticles, one by one, on the five substrates of

TABLE V. Activation energy barriers (eV) of single-adatom hopping in heterodiffusions on flat surface.

Surface	Adatom	Substrate atom					
		Ni	Cu	Pd	Ag	Pt	Au
[110] hopping on (001)	Ni	0.376	0.439	0.566	0.529	0.686	0.591
	Cu	0.407	0.477	0.558	0.569	0.615	0.547
	Pd	0.492	0.566	0.621	0.674	0.627	0.582
	Ag	0.347	0.393	0.459	0.467	0.508	0.437
	Pt	0.706	0.874	0.986	1.189	0.875	0.994
	Au	0.489	0.554	0.590	0.662	0.567	0.531
[11 $\bar{2}$] hopping on (111)	Ni	0.061	0.045	0.087	0.071	0.114	0.078
	Cu	0.050	0.043	0.091	0.078	0.111	0.089
	Pd	0.045	0.041	0.109	0.087	0.128	0.111
	Ag	0.038	0.034	0.074	0.064	0.090	0.075
	Pt	0.018	0.009	0.127	0.040	0.171	0.113
	Au	0.038	0.039	0.110	0.088	0.122	0.117
[1 $\bar{1}$ 0] hopping on (110)	Ni	0.314	0.244	0.369	0.268	0.463	0.313
	Cu	0.334	0.244	0.315	0.249	0.363	0.243
	Pd	0.426	0.318	0.384	0.337	0.402	0.281
	Ag	0.334	0.254	0.333	0.280	0.376	0.262
	Pt	0.308	0.376	0.520	0.492	0.495	0.393
	Au	0.440	0.333	0.392	0.360	0.386	0.276

different species. These heterodiffusion processes are repeated for each of the three surface orientations. These computations are motivated from heteroepitaxial growth. The calculated energy barriers are presented in Table V along with the previous self-diffusion results for comparison purposes. Some results of note are summarized as follows.

On (001) surfaces, Ag can jump more frequently than any other elements on all species of substrates, while Pt should overcome the highest barrier than others on all substrates. Furthermore, all adatoms experience their lowest hopping barriers commonly on a Ni substrate, whereas the highest barrier cases are half shared by Ag and Pt substrates. On (111) surfaces, the energy barriers range from 0.01 to 0.17 eV. The hopping barriers for all adatoms are the highest on a Pt substrate, while all of the adparticles can most easily jump on a Cu surface except for Au hopping adatom. In the in-channel hopping moves on (110) surfaces, Pt meets a higher energy barrier than other adatoms, on all substrate species except Ni. On a Ni substrate, the highest barrier is obtained for a Au atom. On the other hand, Cu can hop more easily than any other adparticles, on all (110) surfaces, except Ni substrate on which Pt atom has the lowest.

E. Other examples

One of the important diffusing events of a single adatom is the long jump that a single atom moves several atomic

spacings by only one jumping movement. It has been well known that the long jump is favored when the most probable diffusion path is a straight line.^{25,69,70} Obviously, such a long jump is less likely than the single hopping in the current systems considered. For example, under scanning tunneling microscopy study, the barrier for the double jump of a Pt adatom is 0.89 eV, which is slightly higher than 0.81 eV for the single jump in the missing row on the (1 \times 2) reconstructed Pt (110) substrate.^{25,70} However, the activation energy of a long jump is the same as that of the associated single atomic-spacing jump, which limits the availability of the energetics approach to the study of long-jump diffusion. In order to calculate the exact diffusion rate of a long jump, we should consider the aforementioned prefactor and the energy barrier together in the context of nonadiabatic coupling of adatom and substrate excitation, which is beyond the current scope.

Another interesting mechanism in single-adatom diffusion is the multiple exchange.⁷¹⁻⁷⁴ It implies the simultaneous exchange movements of several atoms in which the adatom appears to travel a longer distance than what it actually does. For instance, let us consider Cu (001) substrate. In high-temperature molecular dynamics simulations, some atoms are thermally activated simultaneously and move together like multiple exchange. During this process, a metastable state, in which two substrate atoms are thermally activated together, has been observed. It has also been reported that the

TABLE VI. Activation energy barriers (eV) of single-vacancy diffusion on the (001) surface.

Surface	Mechanism	Ni	Cu	Pd	Ag	Pt	Au
(001)	Hopping [110]	0.243	0.445	0.647	0.466	0.931	0.573
		0.562 ^a	0.437 ^a	0.572 ^a	0.417 ^a	0.773 ^a	0.520 ^a
	Hurdling [100]	1.800	1.422	1.266	1.118	1.507	0.772
	Kicking [100]	1.277	0.861	0.900	0.748	1.122	0.605

^aEM in Ref. 64.

energy barrier for this type of multiple exchange is much higher than that for the single exchange.⁷¹

We here present the ADMD simulation of a multiple-exchange process for Cu, as shown in Fig. 6. According to our results, the diffusive movement of multiple exchange is not the simultaneous activation of several atoms but a sequence of individual exchange processes just like wave propagation. Recall that ADMD calculation is to search the minimum-energy path. Therefore, the event in which several substrate atoms are simultaneously in excited motion is most probably excluded from ADMD computation because it is a process of high energy barrier, as reported in the above mentioned high-temperature molecular dynamics simulations. The energy profile of multiple exchange for Cu in the (001) model is given in Fig. 6. Each saddle point has the same energy value. Note that this discussion is good for the multiple exchanges involving a single adatom only. The multiple exchange by the collective motion of two or more adparticles is a separate issue and will be discussed in the following section.

Vacancy-mediated surface diffusion is also of importance (e.g., Refs. 64 and 75–77). We demonstrate the ADMD simulation of single-vacancy diffusive motion on the (100) substrate. Three different pathways are examined. They are hopping, hurdling, and kicking, as named in Fig. 7. In hopping, one neighboring atom moves to the vacancy site, resulting in the vacancy shift to the neighboring site. In hurdling, one of the second-nearest atoms hurdles over the nearest atom to fill the vacancy. In kicking, one of the second-nearest atoms pushes up an atom underneath to fill the vacancy. Three motions are respectively simulated in Fig. 7. The final positions

of vacancy resulting from hurdling and kicking are the same as each other.

Activation energy barriers for the above three vacancy-hopping processes on the (001) surfaces of the six metallic species are tabulated in Table VI. The vacancy-hopping barriers by the effective medium theory⁶⁴ are listed for comparison. We conclude that, for all models, hopping is the dominant mechanism and hurdling is the least probable one. For Cu, energy barriers for hopping, hurdling, and kicking are 0.44, 1.42, and 0.86 eV, respectively, which means that relative diffusion rates of hurdling and kicking to hopping at room temperature (298 K) are, respectively, 10^{-17} s^{-1} and 10^{-7} s^{-1} under the assumption that the prefactors are 10^{13} for all cases. From the calculation by a dimer method using EAM potential, the energy barrier for single-vacancy hopping on the Cu (001) surface is reported to be 0.453 eV,⁷⁷ which is nearly equal to the present result and to a GGA calculation of 0.42 eV.³⁰ Energy barriers of vacancy hopping is slightly higher than those of the adatom hopping for Pd, Pt, and Au, and much lower for Ni. For Ag, the vacancy hopping is as probable as the adatom hopping on this (100) surface because the diffusion barriers are equivalent in the two cases (~ 0.466 eV).

IV. CORRELATED DIFFUSION ON FLAT SUBSTRATES

Another important diffusion mechanism is the correlated diffusion where a few atoms move collectively or corporatively to reduce the activation energy. Concerted jump, dissociation-reassociation,⁷⁸ and leapfrog,^{79,80} mechanisms are among the reported examples. In this section, two, three,

TABLE VII. Activation energy barriers (eV) of correlated diffusion of two adatoms.

Alignment	Mechanism	Ni	Cu	Pd	Ag	Pt	Au
[110] on (001)	Tangential hopping [110]	0.747	0.871	0.963	0.775	1.278	0.731
	Perpendicular hopping [$1\bar{1}0$]	0.376	0.477	0.621	0.467	0.875	0.531
		Exchange [100]	1.351	0.686	0.721	0.615	0.799
[$1\bar{1}0$] on (111)	30° hopping [$1\bar{2}1$]	0.128	0.109	0.150	0.114	0.186	0.100
	90° hopping [$11\bar{2}$]	0.087	0.052	0.119	0.108	0.324	0.229
	Exchange [$\bar{1}\bar{1}2$]	1.635	1.273	1.342	1.202	2.734	1.484
[$1\bar{1}0$] on (110)	In-channel hopping [$1\bar{1}0$]	0.572	0.482	0.671	0.511	0.842	0.456
	Exchange [$1\bar{1}2$]	0.730	0.711	1.136	0.834	1.535	0.906
	Out-channel hopping [001]	1.954	1.838	1.670	1.438	2.140	1.187

and four adparticles are respectively considered to demonstrate the effectiveness of ADMD simulations in facilitating adatom-adatom interactions and associated changes in activation energy barriers. We employ three different surface orientations of (001), (111), and (110) for two- and three-adatom diffusions, while two substrates of (001) and (110) are used for the four-adatom case. On each substrate, two or three different diffusion paths are taken into account. All of the six metallic atoms are considered as before, and only same-species diffusion processes are simulated.

A. Correlated diffusion of two adatoms

In the (001) surface model, two adatoms are initially arranged along the $[110]$ direction. Three different diffusive moves are simulated, as shown in Fig. 8, and their minimum-energy paths and activation energies are computed. Two hopping moves, toward the perpendicular and collinear directions with respect to their original linear alignment, are respectively given in Fig. 8, as well as the exchange process by which two adatoms diffuse to the $[100]$ direction. Calculated activation energy barriers are presented in Table VII. The energy barrier for a perpendicular hopping to $[1\bar{1}0]$ is the same as that of the single-atom hopping. However, collinear (tangential) hopping to $[110]$ needs more energy to occur than the single-atom hopping. In the exchange mechanism, the energy barrier lies around nearly the same values of the single-atom case within variations of 0.02 eV, except for Ni.

On the (111) surface, there exist two immediate hopping paths, which are the moves toward the directions of 30° and 90° , respectively, with respect to the initially aligned direction of the two diffusing particles. They are $[1\bar{2}1]$ and $[11\bar{2}]$ since the two atoms now align along the $[1\bar{1}0]$ direction. The exchange direction is $[\bar{1}\bar{1}2]$, which is normal to the initial alignment of the two adatoms. For Ni, Cu, and Pd, the hopping barriers are increased almost twice in 30° cases, whereas those of 90° hopping moves are increased only by a small amount, both compared with the corresponding single-particle cases. However, Pt and Au cases are the opposite way around, as can be read from Table VII. Ag adatoms result in the significant increases of energy barriers for both hopping directions. The energy barriers of the presumed ex-

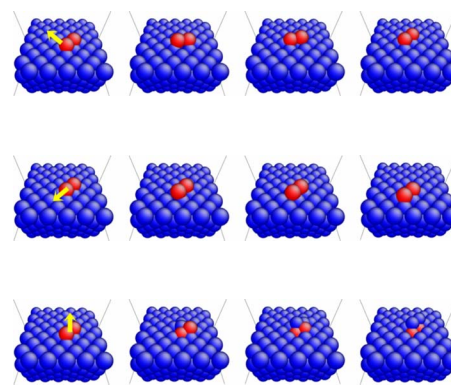


FIG. 8. (Color online) Pathway snapshots of two-adatom diffusion on the (001) surface. Hopping direction is normal to the linear shape (top row). Hopping direction is parallel to the linear shape (middle row). Exchange pathway (bottom row). Each row proceeds from left to right.

change path are nearly the same as the barriers of single-adatom exchange motion, but again, it is not the case of Pt and Au.

On the (110) substrate, two atoms are brought into a line of the in-channel direction $[1\bar{1}0]$ in the initial configuration and then move toward the same direction by hopping. In this case, the activation energy barriers are increased up to almost twice larger values than the single-atom cases, as can be noticed by comparing Table VII with Table I. For example, the energy barrier of the Au dimer is 0.456 eV, which is compatible with the result 0.47 eV by molecular dynamics simulation.⁷⁹ In the case of the Pt dimer, the ADMD result of 1.535 eV is in good agreement with Shiang and Tsong's result of 1.58 eV for exchange, but 0.842 eV for hopping is considerably different from their 1.43 eV hopping energy barrier.⁶⁷ On the other hand, the barriers are raised by the similar amounts for exchange motions.

This variety in the energy barriers of the two-atom diffusions are closely associated with the directions of atoms' initial alignment and subsequent movements. If aligning and moving directions are perpendicular to each other, the energy barriers are nearly the same as the corresponding single-adatom diffusion barriers. However, as the two directions get closer to parallel to each other, activation energy barriers tend to get increased significantly from their single-particle

TABLE VIII. Activation energy barriers (eV) of correlated diffusion of three adatoms.

Alignment	Mechanism	Ni	Cu	Pd	Ag	Pt	Au
$[110]$ on (001)	Hopping $[110]$	1.109	1.256	1.331	1.090	1.740	0.984
	Exchange $[100]$	1.371	0.712	0.766	0.652	0.898	0.512
Triangle on (111)	Hopping	0.172	0.152	0.266	0.185	0.369	0.218
	Exchange	1.873	1.335	1.372	1.159	1.740	1.109
$[1\bar{1}0]$ on (110)	In-channel hopping $[1\bar{1}0]$	0.619	0.718	0.960	0.740	1.195	0.646
	Exchange $[\bar{1}\bar{1}2]$	0.609	0.765	1.071	0.779	1.353	0.756
	Out-channel hopping $[001]$	2.872	2.693	2.455	2.113	3.160	1.763

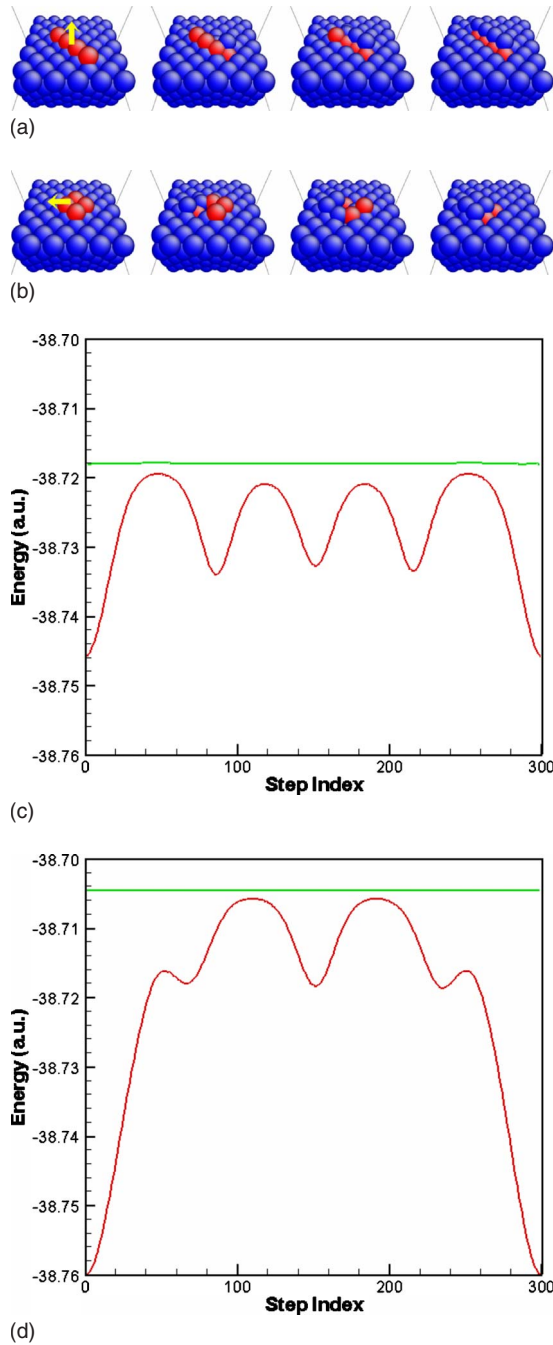


FIG. 9. (Color online) Pathway snapshots and energy profile of four-atom diffusions by exchange. Exchange of linear shape tetramer (a) and exchange of rectangular shape tetramer (b). Each row proceeds from left to right. Energy profiles of linear shape (c) and rectangular shape (d).

counterparts. This is because a diffusing atom hinders the motion of the other atom to participate in the process. For example, the exchange on the (111) surface reveals the same energy barrier as that of one-atom cases, but the barriers of their collinear hopping movements on the (001) surface are almost twice greater than those of single-atom hopping. We will discuss it further in the last part of this section.

B. Correlated diffusion of three adatoms

Possible arrangements of three atoms are collinear and triangular ones. We thus position three adatoms, collinearly on (001) and (110) substrates and triangularly on the (111) surface, considering the atomic structure of the surfaces. On the (001) surface, adatoms are located linearly along the $[110]$ direction at the initial state. They hop to the direction of alignment. Calculated activation energy barriers are given in Table VIII. The energy barriers are fairly increased from those of single-atom hoppings to the same direction. For example, the hopping barrier of Cu is 1.26 eV, while its single-atom movement is 0.48 eV. On the other hand, in the correlated exchange motions to the $[100]$ direction, the energy barrier increases of all species are slight.

In in-channel hopping of three collinear atoms on the (110) substrate, energy barriers elevate considerably for all species except Ni because the moving direction is the same as the initial $[1\bar{1}0]$ alignment. For instance, the barrier of Cu increases from 0.49 eV of two-atom hopping up to 0.72 eV for the current three-atom case. However, in the exchange movements to the $[1\bar{1}2]$ direction, the activation energy barriers are slightly lower than the corresponding two-atom exchange motions, except for Cu.

In the model of the (111) surface, three atoms are initially located in a noncollinear fashion. The activation energy barriers are increased to some extent commonly for both cases of hopping and exchange, compared with the cases of two-atom motions. For example, the Cu barriers for hopping and exchange of three atoms increase up to 0.15 and 1.34 eV, respectively, as shown in Table VIII.

In our previous preliminary work,⁹ we have simulated three Cu adatoms of triangular arrangement in order to demonstrate the feasibility of the ADMD calculation for the analysis of atomic diffusions. Three atoms made a triangle on the (001) surface for initial and final configurations, which are mirror images with respect to each other. In hopping diffusion, an atom climbs over the centerline connecting the other two atoms. On the other hand, the atom kicks a substrate atom out to replace it in exchange move. In this case, we have shown that the exchange takes place due to its lower energy barrier than the hopping. The activation energy barrier of the hopping was higher by 0.30 eV.

C. Correlated diffusion of four adatoms

We now consider the correlated motions of four-atom diffusions where the adatoms are linearly aligned at the initial model in (001) and (110) substrates. Results are summarized in Table IX. On the (001) surface, the energy barriers for collinear hoppings of four atoms along their initially aligned $[110]$ direction are increased due to the reason mentioned previously. One exceptional case is Ni, where the activation energy barrier is rather decreased. In this case, Ni atoms do hop, not cooperatively but individually, atom by atom.

In in-channel hopping of four adparticles on the (110) substrate, as the number of atoms increases, energy barriers increase as well. This time, the in-channel hopping direction is collinear, i.e., $[1\bar{1}0]$ direction, so that the barriers are ex-

TABLE IX. Activation energy barrier (eV) of correlated diffusion of four adatoms.

Alignment	Mechanism	Ni	Cu	Pd	Ag	Pt	Au
[110] on (001)	Hopping [110]	0.748	1.615	1.661	1.376	2.132	1.185
	Exchange [100]	1.347	0.718	0.786	0.675	0.945	0.547
[1 $\bar{1}$ 0] on (110)	In-channel hopping [1 $\bar{1}$ 0]	0.630	0.985	1.275	0.985	1.578	0.847
	Exchange [1 $\bar{1}$ 2]	0.626	0.777	1.070	1.002	1.353	0.989
	Out-channel hopping [001]	3.850	3.653	3.521	3.117	4.723	2.902

pected to increase. For Cu, the activation energy barriers are 0.24, 0.49, 0.74, and 0.99 eV, which respectively correspond to one-, two-, three-, and four-adatom in-channel hoppings. However, the energy barriers for exchange motions remain in comparable ranges as the number of adatom increases, for all species but Au.

An additional calculations of four-adatom exchange motions are conducted to compare the collinear and rectangular initial arrangements on the (001) substrate. The minimum-energy paths and the activation energy barriers during the two exchange motions are shown in Fig. 9. In the collinear case, the potential-energy profile shows four nearly equivalent energy barriers, and these four values are approximately the same as the activation energy barrier of the single-atom exchange. In contrast, the rectangular arrangement case results in a higher energy barrier because the atoms located at the front in the diffusing direction hinder the exchange motions of the rest of the adatoms behind.

D. Remarks on correlated diffusions

The activation energy barrier is closely linked with the directional property in models. Two directions are relevant: one is the initial alignment direction of multiple adatoms, and the other is the direction of their movements, as previously mentioned in the two-adatom case. For example, let us consider the collinear hopping of two or more atoms initially located collinearly on the (100) flat surface. The energy barriers of their hopping movements increase proportionally to the number of diffusing atoms. This trend can also be found in other EAM simulations of concerted jump on the (110) (2×1) surface.⁸¹ The atom located ahead hinders the hopping moves of the other atom behind. Consequently, the energy barriers increase when multiple adatoms diffuse by collinear hopping mechanism. In the perpendicular hopping where the hopping direction is normal to the initial linear alignment, there is no increased obstacle in their diffusion paths. This implies that collinearly aligned atoms can easily hop to the normal direction than to the collinear direction. This dependence on the number of atoms in the linked movements can also be found in the in-channel hopping diffusions of multiple adatoms on the (110) surface and in the correlated exchanges of four adatoms on the (001) surface, as shown in Fig. 9.

It is noted that those increases in the activation energy barrier are valid only for the cases of correlated diffusions. If adatoms move to the collinear direction individually with appropriate time intervals, the barrier is equivalent to that of the single-atom diffusion. In this case, we should again return to the prefactor in order to measure the event frequency of diffusions. For example, the collinear hoppings of three and four Ni atoms on the (001) surface have different energy barriers, which depends on whether they diffuse cooperatively or not. In an energetics study, the conclusion we can draw is limited to the proportional increase of activation energy barriers for correlated hopping movements.

V. CONCLUDING REMARKS

We have applied the action-derived molecular dynamics to the simulations of diverse diffusion processes on flat fcc metal surfaces. ADMD is the action-based numerical technique to search minimum-energy paths and the associated activation energy barriers for structural transition when the initial and final atomic configurations are known *a priori*. The method is here demonstrated to be effective for a route-specific analysis of diffusion mechanism. ADMD results on basic diffusive movements of a single adatom have been compared with other experiments and calculations in literature. More complex situations, such as multiple adatom's collective motion, can also be analyzed by ADMD and have thus been presented in this paper. In the companion paper (Part II),⁴ we present the ADMD simulation of diffusion mechanism associated with surface steps, including, for example, jumps over a double-layered step, which is very difficult to be facilitated by the conventional molecular dynamics simulation.

ACKNOWLEDGMENTS

S.Y.K. was supported by the Korea Advanced Institute of Science and Technology. I.-H.L. acknowledges support by the Ministry of Commerce, Industry, and Energy of Korea through "The R&D Project for Key Technology." S.J. was supported by the University of Wyoming. The authors would like to thank Eunyoung Cho for her help in preparing the manuscript.

- *Author to whom correspondence should be addressed; sjun@uwoyo.edu
- ¹A. F. Voter, F. Montalenti, and T. C. Germann, *Annu. Rev. Mater. Res.* **32**, 321 (2002).
 - ²T. Ala-Nissia, R. Ferrando, and S. C. Ying, *Adv. Phys.* **51**, 949 (2002).
 - ³D. Passerone and M. Parrinello, *Phys. Rev. Lett.* **87**, 108302 (2001).
 - ⁴S. Y. Kim, I.-H. Lee, and S. Jun, following paper, *Phys. Rev. B* **76**, 245408 (2007).
 - ⁵D. Passerone, M. Ceccarelli, and M. Parrinello, *J. Chem. Phys.* **118**, 2025 (2003).
 - ⁶I.-H. Lee, J. Lee, and S. Lee, *Phys. Rev. B* **68**, 064303 (2003).
 - ⁷Y.-H. Kim, I.-H. Lee, K. J. Chang, and S. Lee, *Phys. Rev. Lett.* **90**, 065501 (2003).
 - ⁸D. Aktah, D. Passerone, and M. Parrinello, *J. Phys. Chem. A* **108**, 848 (2004).
 - ⁹I.-H. Lee, S. Y. Kim, and S. Jun, *Comput. Methods Appl. Mech. Eng.* **193**, 1633 (2004).
 - ¹⁰I.-H. Lee, H. Kim, and J. Lee, *J. Chem. Phys.* **120**, 4672 (2004).
 - ¹¹I.-H. Lee, S.-Y. Kim, and J. Lee, *Chem. Phys. Lett.* **412**, 307 (2005).
 - ¹²M. Ceccarelli, F. Mercuri, D. Passerone, and M. Parrinello, *J. Phys. Chem. B* **109**, 17094 (2005).
 - ¹³I.-H. Lee, S. Jun, H. Kim, S. Y. Kim, and Y. Lee, *Appl. Phys. Lett.* **88**, 011913 (2006).
 - ¹⁴S. Pendurti, S. Jun, I.-H. Lee, and V. Prasad, *Appl. Phys. Lett.* **88**, 201908 (2006).
 - ¹⁵S. Y. Kim, I.-H. Lee, S. Jun, Y. Lee, and S. Im, *Phys. Rev. B* **74**, 195409 (2006).
 - ¹⁶F. Cleri and V. Rosato, *Phys. Rev. B* **48**, 22 (1993).
 - ¹⁷N. I. Papanicolaou, *Comput. Mater. Sci.* **24**, 117 (2002).
 - ¹⁸G. L. Kellogg, *Surf. Sci. Rep.* **21**, 1 (1994).
 - ¹⁹S. Durukanoglu, O. S. Trushin, and T. S. Rahman, *Phys. Rev. B* **73**, 125426 (2006).
 - ²⁰J. Li, *Modell. Simul. Mater. Sci. Eng.* **11**, 173 (2003).
 - ²¹C. L. Liu, J. M. Cohen, J. B. Adams, and A. F. Voter, *Surf. Sci.* **253**, 334 (1991).
 - ²²L. S. Perkins and A. E. DePristo, *Surf. Sci.* **325**, 169 (1995).
 - ²³J. Merikoski, I. Vattulainen, J. Heinonen, and T. Ala-Nissila, *Surf. Sci.* **387**, 167 (1997).
 - ²⁴K.-D. Shiang, *J. Chem. Phys.* **99**, 9994 (1993).
 - ²⁵F. Montalenti and R. Ferrando, *Phys. Rev. B* **59**, 5881 (1999).
 - ²⁶U. Kürpick, *Phys. Rev. B* **64**, 075418 (2001).
 - ²⁷U. Kürpick and T. S. Rahman, *Phys. Rev. B* **57**, 2482 (1998).
 - ²⁸W. Xiao, P. A. Greaney, and D. C. Chrzan, *Phys. Rev. B* **70**, 033402 (2004).
 - ²⁹A. V. Evteev, A. T. Kosilov, and S. A. Solyanik, *Phys. Solid State* **46**, 1781 (2004).
 - ³⁰G. Boisvert and L. J. Lewis, *Phys. Rev. B* **56**, 7643 (1997).
 - ³¹C. Lee, G. T. Barkema, M. Breeman, A. Pasquarello, and R. Car, *Surf. Sci.* **306**, L575 (1994).
 - ³²B. D. Yu and M. Scheffler, *Phys. Rev. Lett.* **77**, 1095 (1996).
 - ³³G. Boisvert, L. J. Lewis, M. J. Puska, and R. M. Nieminen, *Phys. Rev. B* **52**, 9078 (1995).
 - ³⁴P. J. Feibelman, *Phys. Rev. B* **64**, 125403 (2001).
 - ³⁵B. D. Yu and M. Scheffler, *Phys. Rev. B* **56**, R15569 (1997).
 - ³⁶R. T. Tung and W. R. Graham, *Surf. Sci.* **97**, 73 (1980).
 - ³⁷P. Schrammen and J. Hölzl, *Surf. Sci.* **130**, 203 (1983).
 - ³⁸J. J. de Miguel, A. Sánchez, A. Cebollada, J. M. Callego, J. Ferrón, and S. Ferrer, *Surf. Sci.* **189-190**, 1062 (1987).
 - ³⁹M. Breeman and D. O. Boerma, *Surf. Sci.* **269-270**, 224 (1992).
 - ⁴⁰H.-J. Ernst, F. Fabre, and J. Lapujoulade, *Phys. Rev. B* **46**, 1929 (1992).
 - ⁴¹H. Dürr, J. F. Wendelken, and J.-K. Zuo, *Surf. Sci.* **328**, L527 (1995).
 - ⁴²J. W. Evans, D. K. Flynn-Sanders, and P. A. Thiel, *Surf. Sci.* **298**, 378 (1993).
 - ⁴³M. H. Langelaar, M. Breeman, and D. O. Boerma, *Surf. Sci.* **352-354**, 597 (1996).
 - ⁴⁴L. Bardotti, M. C. Bartelt, C. J. Jenks, C. R. Stoldt, J.-M. Wen, C.-M. Zhang, P. A. Thiel, and J. W. Evans, *Langmuir* **14**, 1487 (1998).
 - ⁴⁵G. L. Kellogg and P. J. Feibelman, *Phys. Rev. Lett.* **64**, 3143 (1990).
 - ⁴⁶C. M. Chang, C. M. Wei, and S. P. Chen, *Phys. Rev. Lett.* **85**, 1044 (2000).
 - ⁴⁷Y. Li and A. E. DePristo, *Surf. Sci.* **351**, 189 (1996).
 - ⁴⁸H. Bulou and C. Massobrio, *Phys. Rev. B* **72**, 205427 (2005).
 - ⁴⁹M. I. Haftel, *Phys. Rev. B* **64**, 125415 (2001).
 - ⁵⁰G. Boisvert, L. J. Lewis, and A. Yelon, *Phys. Rev. Lett.* **75**, 469 (1995).
 - ⁵¹M. Villarba and H. Jónsson, *Surf. Sci.* **317**, 15 (1994).
 - ⁵²R. Wang and K. A. Fichthorn, *Surf. Sci.* **301**, 253 (1994).
 - ⁵³C. Ratsch and M. Scheffler, *Phys. Rev. B* **58**, 13163 (1998).
 - ⁵⁴C. Ratsch, A. P. Seitsonen, and M. Scheffler, *Phys. Rev. B* **55**, 6750 (1997).
 - ⁵⁵P. J. Feibelman, J. S. Nelson, and G. L. Kellogg, *Phys. Rev. B* **49**, 10548 (1994).
 - ⁵⁶G. Boisvert, L. J. Lewis, and M. Scheffler, *Phys. Rev. B* **57**, 1881 (1998).
 - ⁵⁷P. J. Feibelman, *Phys. Rev. Lett.* **81**, 168 (1998).
 - ⁵⁸J. Repp, F. Moresco, G. Meyer, K.-H. Rieder, P. Hyldgaard, and M. Persson, *Phys. Rev. Lett.* **85**, 2981 (2000).
 - ⁵⁹A. Steltenpohl and N. Memmel, *Surf. Sci.* **454-456**, 558 (2000).
 - ⁶⁰H. Brune, K. Bromann, H. Röder, K. Kern, J. Jacobsen, P. Stoltze, K. Jacobsen, and J. Nørskov, *Phys. Rev. B* **52**, R14380 (1995).
 - ⁶¹G. W. Jones, J. M. Marcano, J. K. Nørskov, and J. A. Venables, *Phys. Rev. Lett.* **65**, 3317 (1990).
 - ⁶²M. Bott, M. Hohage, M. Morgenstern, T. Michely, and G. Comsa, *Phys. Rev. Lett.* **76**, 1304 (1996).
 - ⁶³K. Kyuno, A. Götzhäuser, and G. Ehrlich, *Surf. Sci.* **397**, 191 (1998).
 - ⁶⁴P. Stoltze, *J. Phys.: Condens. Matter* **6**, 9495 (1994).
 - ⁶⁵L. S. Perkins and A. E. DePristo, *Surf. Sci.* **317**, L1152 (1994).
 - ⁶⁶D. W. Bassett and P. R. Webber, *Surf. Sci.* **70**, 520 (1978).
 - ⁶⁷K.-D. Shiang and T. T. Tsong, *Phys. Rev. B* **51**, 5522 (1995).
 - ⁶⁸S. Cünther, A. Hitzke, and R. J. Behm, *Surf. Rev. Lett.* **4**, 1103 (1997).
 - ⁶⁹L. Y. Chen, M. R. Baldan, and S. C. Ying, *Phys. Rev. B* **54**, 8856 (1996).
 - ⁷⁰T. R. Linderoth, S. Horch, E. Lægsgaard, I. Stensgaard, and F. Besenbacher, *Phys. Rev. Lett.* **78**, 4978 (1997).
 - ⁷¹J. E. Black and Z.-J. Tian, *Phys. Rev. Lett.* **71**, 2445 (1993).
 - ⁷²J. M. Cohen, *Surf. Sci.* **306**, L545 (1994).
 - ⁷³G. A. Evangelakis and N. I. Papanicolaou, *Surf. Sci.* **347**, 376 (1996).
 - ⁷⁴R. Ferrando, *Phys. Rev. Lett.* **76**, 4195 (1996).
 - ⁷⁵R. van Gastel, E. Somfai, S. B. van Albada, W. van Saarloos, and J. W. M. Frenken, *Phys. Rev. Lett.* **86**, 1562 (2001).

- ⁷⁶R. van Gastel, E. Somfai, S. B. van Albada, W. van Saarloos, and J. W. M. Frenken, *Surf. Sci.* **521**, 10 (2002).
- ⁷⁷M. Basham, P. A. Mulheran, and F. Montalenti, *Surf. Sci.* **565**, 289 (2004).
- ⁷⁸T. R. Linderoth, S. Horch, L. Petersen, S. Helveg, M. Schønning, E. Lægsgaard, I. Stensgaard, and F. Besenbacher, *Phys. Rev. B* **61**, R2448 (2000).
- ⁷⁹T. R. Linderoth, S. Horch, L. Petersen, S. Helveg, E. Lægsgaard, I. Stensgaard, and F. Besenbacher, *Phys. Rev. Lett.* **82**, 1494 (1999).
- ⁸⁰F. Montalenti and R. Ferrando, *Phys. Rev. Lett.* **82**, 1498 (1999).
- ⁸¹U. Kürpick, *Phys. Rev. B* **63**, 045409 (2001).